JOURNAL OF BACTERIOLOGY, Oct. 2010, p. 5115–5123 Vol. 192, No. 19
0021-9193/10/$12.00 doi:10.1128/JB.00612-10

$NADP^+$ Reduction with Reduced Ferredoxin and $NADP^+$ Reduction with NADH Are Coupled via an Electron-Bifurcating Enzyme Complex in *Clostridium kluyveri*[▽]

Shuning Wang,‡ Haiyan Huang,‡ Johanna Moll, and Rudolf K. Thauer*

Max Planck Institute for Terrestrial Microbiology, D-35043 Marburg, Germany

Received 28 May 2010/Accepted 24 July 2010

It was recently found that the cytoplasmic butyryl-coenzyme A (butyryl-CoA) dehydrogenase-EtfAB complex from *Clostridium kluyveri* couples the exergonic reduction of crotonyl-CoA to butyryl-CoA with NADH and the endergonic reduction of ferredoxin with NADH via flavin-based electron bifurcation. We report here on a second cytoplasmic enzyme complex in *C. kluyveri* capable of energetic coupling via this novel mechanism. It was found that the purified iron-sulfur flavoprotein complex NfnAB couples the exergonic reduction of $NADP^+$ with reduced ferredoxin (Fd_{red}) and the endergonic reduction of $NADP^+$ with NADH in a reversible reaction: $Fd_{red}^{2-} + NADH + 2\ NADP^+ + H^+ = Fd_{ox} + NAD^+ + 2\ NADPH$. The role of this energy-converting enzyme complex in the ethanol-acetate fermentation of *C. kluyveri* is discussed.

Clostridium kluyveri is unique in fermenting ethanol and acetate to butyrate, caproate, and H_2 (reaction 1) and in deriving a large (30%) portion of its cell carbon from CO_2. Both the energy metabolism and the pathways of biosynthesis have therefore been the subject of many investigations (for relevant literature, see references 12 and 27).

$$6\ \text{ethanol} + 3\ \text{acetate}^- \rightarrow 3\ \text{butyrate}^- + 1\ \text{caproate}^- + 1\ H^+ + 4\ H_2O + 2\ H_2;\ \Delta G^{0\prime} = -183.5\ \text{kJ/mol}\ H^+ \quad (1)$$

During growth of *C. kluyveri* on ethanol and acetate, approximately five ethanol and four acetate molecules are converted to three butyrate molecules and one caproate molecule (reaction 1a), and one ethanol molecule is oxidized to one $acetate^-$, one H^+, and two H_2 (reaction 1b) molecules (23, 31). How exergonic reaction 1a is coupled with endergonic reaction 1b and with ATP synthesis from ADP and P_i ($\Delta G^{o\prime} = +32$ kJ/mol) has remained unclear for many years.

$$5\ \text{ethanol} + 4\ \text{acetate}^- \rightarrow 3\ \text{butyrate}^- + 1\ \text{caproate}^- + 5\ H_2O;\ \Delta G^{0\prime} = -193.2\ \text{kJ/mol} \quad (1a)$$

$$1\ \text{ethanol} + H_2O \rightarrow \text{acetate}^- + H^+ + 2\ H_2;\ \Delta G^{0\prime} = +9.7\ \text{kJ/mol} \quad (1b)$$

We recently showed (12) that, in *Clostridium kluyveri*, the exergonic reduction of crotonyl-coenzyme A (crotonyl-CoA) ($E_o' = -10$ mV) with NADH ($E_o' = -320$ mV) involved in reaction 1a is coupled with the endergonic reduction of ferredoxin (Fd_{ox}) ($E_o' = -420$ mV) with NADH ($E_o' = -320$ mV) involved in reaction 1b via the recently proposed mechanism of flavin-based electron bifurcation (7). The coupling reaction is catalyzed by the cytoplasmic butyryl-CoA dehydrogenase-EtfAB complex (reaction 2) (12):

$$\text{crotonyl-CoA} + 2\ NADH + Fd_{OX} \rightarrow \text{butyryl-CoA} + 2\ NAD^+ + Fd_{red}^{2-};\ \Delta G^{0\prime} = -40\ \text{kJ/mol} \quad (2)$$

The reduced ferredoxin (Fd_{red}^{2-}) is assumed to be used for rereduction of NAD^+ via a membrane-associated, proton-translocating ferredoxin:NAD oxidoreductase (RnfABCDEG) (reaction 3), and the proton motive force thus generated is assumed to drive the phosphorylation of ADP via a membrane-associated F_1F_0 ATP synthetase (reaction 4):

$$Fd_{red}^{2-} + NAD^+ + H^+ = Fd_{OX} + NADH + \Delta\mu H^+ \quad (3)$$

$$ADP + P_i + \Delta\mu H^+ = ATP + H_2O \quad (4)$$

The novel coupling mechanism represented by reactions 2 and 3 allowed for the first time the possibility of formulating a metabolic scheme for the ethanol-acetate fermentation that could account for the observed fermentation products and growth yields and thus for the observed ATP gains (27). One issue, however, remained open, namely, why the formation of butyrate from ethanol and acetate in the fermentation involves both an $NADP^+$- and an NAD^+-specific β-hydroxybutyryl-CoA dehydrogenase (16), considering that, in the oxidative part of the fermentation (ethanol oxidation to acetyl-CoA), only NADH is generated (8, 9, 13).

The presence of a reduced ferredoxin:$NADP^+$ oxidoreductase was proposed based on results of enzymatic studies performed 40 years ago. Cell extracts of *Clostridium kluyveri* were found to catalyze the formation of H_2 from NADPH in a ferredoxin- and NAD^+-dependent reaction (34). The results were interpreted to indicate that *C. kluyveri* contains a ferredoxin-dependent hydrogenase and an NADPH:ferredoxin oxidoreductase with transhydrogenase activity. H_2 formation from NADPH was strictly dependent on the presence of

* Corresponding author. Mailing address: Max Planck Institute for Terrestrial Microbiology, Karl-von-Frisch-Strasse 10, D-35043 Marburg, Germany. Phone: 49 6421 178 101. Fax: 49 6421 178 109. E-mail: thauer@mpi-marburg.mpg.de.

‡ S.W. and H.H. contributed equally to this work.

▽ Published ahead of print on 30 July 2010.

NAD^+ and was inhibited by NADH, inhibition being competitive with the presence of NAD^+, indicating that ferredoxin reduction with NADPH is under the allosteric control of the NAD^+/NADH couple. The cell extracts also catalyzed the NADH-dependent reduction of $NADP^+$ with reduced ferredoxin (21, 34). Purification of the enzyme catalyzing these reactions was not achieved, and no function in the energy metabolism of *C. kluyveri* was assigned.

In this communication, we report on the properties of the recombinant enzyme that catalyzes the NAD^+-dependent reduction of ferredoxin with NADPH and the NADH-dependent reduction of $NADP^+$ with reduced ferredoxin and show that the cytoplasmic heterodimeric enzyme couples the exergonic reduction of $NADP^+$ with reduced ferredoxin with the endergonic reduction of $NADP^+$ with NADH in a fully reversible reaction. The transhydrogenation reaction is endergonic, because in *vivo* the NADH/NAD^+ ratio is generally near 0.3 and the NADPH/$NADP^+$ ratio is generally above 1 (2, 30).

$$Fd_{red}^{2-} + 2\ NADP^+ + NADH + H^+ = Fd_{OX} + 2\ NADPH + NAD^+;\ \Delta G^{0\prime} = -20\ kJ/mol \quad (5)$$

$NADP^+$ reduction is most probably the physiological function of the enzyme, which is why we chose the abbreviation NfnAB (for NADH-dependent reduced ferredoxin:$NADP^+$ oxidoreductase).

MATERIALS AND METHODS

Strains and growth. *C. kluyveri* DSM 555 was grown on acetate-ethanol-bicarbonate medium at 37°C (34). Cells were harvested by the use of a continuous-flow centrifuge at the late exponential phase and stored at −80°C until they were used. *Clostridium pasteurianum* DSM 525 was grown on a glucose-ammonium medium (11), and the cells were harvested at the mid-exponential phase.

Biochemicals. $NADP^+$, NAD^+, NADPH, NADH, glucose-6-phosphate, glucose-6-phosphate dehydrogenase from baker's yeast, triphenyltetrazolium choride (TTC), and benzyl viologen dichloride were obtained from Sigma-Aldrich Chemie GmbH (Taufkirchen, Germany). Lactate dehydrogenase from pig heart was from Roche (Mannheim, Germany). Ferredoxin (24) and ferredoxin-dependent hydrogenase (12) were purified from *C. pasteurianum* DSM 525.

Purification of NfnAB from *C. kluyveri*. Frozen wet cells of *C. kluyveri* (15 g) were suspended in 20 ml of 50 mM MOPS-KOH (morpholinepropanesulfonic acid-KOH) (pH 7.0) containing 10 mM 2-mercaptoethanol and 5 μM flavin adenine dinucleotide (FAD). After the addition of 10 ml of the same buffer containing 25 mg of lysozyme, 5 mg of DNase I, and 30 mM $MgCl_2$, the suspension was incubated at 37°C for 35 min and then centrifuged for 30 min at 40,000 × *g* and 4°C. A brown supernatant was obtained with about 40 mg of protein per ml. The protein content was measured by the Bio-Rad protein assay (Munchen, Germany), with bovine serum albumin as the standard.

The purification was done in an anaerobic tent (Coy, Ann Arbor, MI) filled with 95% N_2 and 5% H_2 and containing a palladium catalyst for O_2 reduction with H_2. The supernatant was applied on an 80-ml Q-Sepharose column equilibrated with 50 mM MOPS-KOH (pH 7.0) containing 2 mM dithiothreitol (DTT) and 5 μM FAD. The column was eluted with a 0 to 1 M NaCl linear gradient. The fractions containing activity were pooled, concentrated, and desalted by the use of an Amicon cell with a 10-kDa-cutoff membrane. The concentrate was then loaded on a 30-ml Blue Sepharose column equilibrated with the same buffer and was eluted stepwise with an NaCl step gradient (50 ml each of 0, 0.2, 0.4, 0.6, and 1 M NaCl). After being subjected to concentration and desalting, the fractions with activity were pooled and applied on a 10-ml hydroxyapatite column equilibrated with 10 mM potassium phosphate (pH 7.0) containing 2 mM DTT and 5 μM FAD. The column was eluted with a 0 to 0.5 M potassium phosphate (pH 7.0) linear gradient. The eluate was concentrated by ultrafiltration and finally applied on a 24-ml Superdex G200 column. Fractions with activity were analyzed by sodium dodecyl sulfate-polyacrylamide gel electrophoresis (SDS-PAGE) and stained with Coomassie brilliant blue. The bands were excised and the polypeptides therein digested with trypsin, analyzed by matrix-assisted laser desorption ionization–time of flight mass spectrometry (MALDI-TOF MS), and identified by a peptide mass fingerprinting (PMF) search in the NCBInr database.

Heterologous expression of *nfnAB*, *nfnA*, and *nfnB*. The genes were amplified by PCR with high-fidelity Phusion DNA polymerase (New England Biolabs GmbH, Frankfurt, Germany) by the use of *C. kluyveri* genomic DNA as a template. The genes were expressed either together or individually where indicated and tagged with a 3′ or 5′ His_6 cassette.

***nfnAB* without a His_6 cassette.** The following primers were used: 5′-GGGTG CATATGATGTATAAAATTGTAGACAAACAAGCTC-3′ (forward primer; the NdeI restriction site is underlined) and 5′-CTAGAACTCGAGTTATTTCT TGCTTAAGTACTCATCTATAGC-3′ (reverse primer; the XhoI restriction site is underlined). The blunt PCR product was ligated into pCR Blunt vector (Invitrogen, Karlsruhe, Germany), which was subsequently transformed into TOP10 cells. After amplification, the construct was digested by the use of NdeI and XhoI, and the target fragment was ligated into expression vector pET24b(+), which had been digested by the same restriction endonucleases. The new construct was introduced into TOP10 again and verified by DNA sequencing. It was then transformed into *Escherichia coli* BL21(DE3) for expression.

***nfnAB* with an *nfnA* 5′ His_6 cassette.** The following primers were used: 5′-C ACCATGTATAAAATTGTAGAC-3′ (forward primer; CACC was used for directional cloning) and 5′-TTATTTCTTGCTTAAGTACTC-3′ (reverse primer). The PCR product was cloned into pET200/D-TOPO (Invitrogen), and the construct was subsequently transformed into One-Shot TOP10 *E. coli* (Invitrogen). After verifying the DNA sequence, the constructs were transformed into *E. coli* BL21 Star (DE3) (Invitrogen) and expressed.

***nfnAB* with an *nfnB* 3′ His_6 cassette.** The procedure was the same that used for cloning *nfnAB* without a His_6 cassette except for the use of a different reverse primer: 5′-CTAGAACTCGAGTTTCTTGCTTAAGTACTCATCTATAGC-3′ (the XhoI restriction site is underlined).

***nfnAB* with both an *nfnA* 5′ His_6 cassette and an *nfnB* 3′ His_6 cassette.** The procedure was same as that used for cloning *nfnAB* without a His_6 cassette except for the use of different primers and a different expression vector. The forward primer used was 5′-GGGTGCATATGATGTATAAAATTGTAGACAAACA AGCTC-3′ (the NdeI restriction site is underlined), and the reverse primer was the same as that used for cloning *nfnAB* with an *nfnB* 3′ His_6 cassette. The expression vector was pET28b(+).

***nfnA* with a 5′ His_6 cassette.** The procedure was same as that used for cloning *nfnAB* with an *nfnA* 5′ His_6 cassette except for the use of a different reverse primer: 5′-TTATTTGTCACCTCCGCA-3′.

***nfnB* with a 5′ His_6 cassette.** The procedure was the same as that used for cloning *nfnAB* with an *nfnA* 5′ His_6 cassette except for the use of a different forward primer: 5′-CACCATGGCTGTAGATAGAATG-3′ (CACC was used for directional cloning).

For expression, the cells were aerobically grown in 2 liters of tryptone-phosphate medium at 37°C with a high stirring speed (750 rpm). When an optical density at 600 nm (OD_{600}) of about 2.2 was reached, the temperature was lowered to room temperature and the stirring speed lowered to 250 rpm. Concomitantly, the culture was supplemented with IPTG (isopropyl β-D-thiogalactopyranoside [0.5 mM]) to induce gene expression and with cysteine (0.12 g $liter^{-1}$), ferrous sulfate (0.1 g $liter^{-1}$), ferric citrate (0.1 g $liter^{-1}$), and ferric ammonium citrate (0.1 g $liter^{-1}$) for the enhancement of iron-sulfur cluster synthesis. After 20 h, stirring was stopped and the culture was left for another 20 h at room temperature before being harvested by centrifugation. The recombinant *E. coli* cells were washed with anaerobic 50 mM MOPS-KOH (pH 7.0) and stored at −80°C in an N_2 atmosphere until they were used.

Purification of His-tagged proteins. The purification steps were performed under strictly anoxic conditions. The *E. coli* cells were resuspended in buffer A (50 mM NaH_2PO_4, 300 mM NaCl, 10 mM imidazole [pH 8.0]) and disrupted by sonication (six times at 32 W for 6 min each time). Cell debris was removed by centrifugation at 40,000 × *g* and 4°C for 30 min. The supernatant was applied on a 30-ml nickel-nitrilotriacetic acid (Ni-NTA) Superflow column (Qiagen, Hilden, Germany). The recombinant protein was eluted with buffer B (50 mM NaH_2PO_4, 300 mM NaCl, 250 mM imidazole [pH 8.0]) in a programmed gradient (90 ml at 10 mM, 60 ml at 25 mM, 90 ml at 35 mM, and 150 ml at 35 mM to 250 mM). The purified protein was concentrated by ultrafiltration, washed with 50 mM MOPS-KOH (pH 7.0) containing 2 mM DTT and 5 μM FAD, and then stored at −20°C in an N_2 atmosphere until use.

FeS cluster reconstitution and determination of iron content. In order to improve the activity of the purified proteins, their FeS clusters were reconstituted *in vitro*. The reaction mixture contained 100 mM Tris-HCl (pH 7.4), 8 mM DTT, 10 μM FAD, 2 mg of enzyme ml^{-1}, 2 mM cysteine, and 1.5 mM $FeSO_4$. The reaction was performed at room temperature for 1 h under strictly anoxic con-

ditions. After centrifugation at 52,000 × *g* and 4°C for 30 min, the supernatant was ultrafiltrated by the use of an Amicon filter (Millipore) (30-kDa cutoff) and washed with 5 volumes of 100 mM Tris-HCl buffer (pH 7.4).

The iron content of the enzyme was determined colorimetrically with 3-(2-pyridyl)-5,6-bis(5-sulfo-2-furyl)-1,2,4-triazinedisodium trihydrate (Ferene), with Mohr's salt used as the standard according to a method previously described (3, 20).

Enzyme activity assays. Except where indicated, these were performed at 37°C in 1-ml anaerobic cuvettes closed with a rubber stopper and filled with 0.8-ml reaction mixtures and 0.2 ml of N_2 or H_2 at 1.2×10^5 Pa. The reaction mixtures contained 100 mM MOPS-KOH (pH 7.0), 10 mM 2-mercaptoethanol, and 12 μM FAD as basal ingredients.

TTC reduction with NADPH. The basal reaction mixture was supplemented with 0.5 mM NADP$^+$, 40 mM glucose-6-phosphate, and 2 U of glucose-6-phosphate dehydrogenase (NADPH regeneration system), 2 mM NAD$^+$, and 0.4 mM TTC. N_2 was used for the gas phase. The reaction was started with enzyme, and TTC reduction was followed using photometrical observations at 546 nm (ε = 9.1 mM^{-1} cm^{-1}). Reduction of 1 μmol of TTC per min was defined as representing 1 unit.

NAD$^+$ reduction with NADPH. The basal reaction mixture was supplemented with an NADPH regeneration system, 10 mM NAD$^+$, 10 μM ferredoxin, and 1 U of hydrogenase. N_2 was used for the gas phase. The reaction was started with enzyme, and NAD$^+$ reduction was followed using photometrical observations at 380 nm (ε = 1.2 mM^{-1} cm^{-1}). Formation of 1 μmol of NADH per min was defined as representing 1 unit.

NADP$^+$ reduction with reduced ferredoxin. The basal reaction mixture was supplemented with 2 mM NADP$^+$ (or as indicated), 0.75 mM NADH (or as indicated), 30 μM ferredoxin, and 1 U of hydrogenase. H_2 was used for the gas phase. The reaction was started with enzyme, and NADP$^+$ reduction was followed using photometrical observations at 380 nm (ε = 1.2 mM^{-1} cm^{-1}). Formation of 1 μmol of NAD(P)H per min was defined as 1 unit.

Ferredoxin reduction with NADPH. The basal reaction mixture was supplemented with an NADPH regeneration system, 10 mM NAD$^+$ and 50 μM ferredoxin. N_2 was used for the gas phase. The reaction was started with enzyme, and ferredoxin reduction was followed by photometrical observations at 430 nm ($\varepsilon_{\Delta ox\text{-}red} \approx$ 13.1 mM^{-1} cm^{-1}). Reduction of 1 μmol of ferredoxin per min was defined as representing 1 unit.

Benzyl viologen reduction with NADPH or NADH. When NADPH was used as electron donor, the basal reaction mixture was supplemented with an NADPH regeneration system and 1 mM benzyl viologen. When NADH was used as an electron donor, the basal reaction mixture was supplemented with 1 mM NADH and 1 mM benzyl viologen. N_2 was used for the gas phase. The reaction was started with enzyme, and benzyl viologen reduction was followed by photometrical observations at 578 nm (ε = 7.8 mM^{-1} cm^{-1}). Reduction of 1 μmol of benzyl viologen per min was defined as representing 1 unit.

H_2 formation. Where indicated, ferredoxin reduction was coupled with the hydrogenase reaction and gas chromatography was used to measure the H_2 that was produced. The assays were performed at 37°C using 6.5-ml serum bottles closed with a rubber stopper and containing 0.8 ml of reaction mixture consisting of 100 mM MOPS-KOH (pH 7.0), 10 mM 2-mercaptoethanol, 12 μM FAD, 30 μM ferredoxin, 1 U of hydrogenase, and 0.27 mg of NfnAB as basal components. The 5.7-ml gas phase was composed of N_2 at 1.2×10^5 Pa. Where indicated, the reaction mixture additionally contained an NADPH regeneration system (2 mM NADP$^+$, 40 mM glucose-6-phosphate, and 2 U of glucose-6-phosphate dehydrogenase) and NAD$^+$ in various amounts or an NAD$^+$ regeneration system (2 mM NAD$^+$, 20 mM pyruvate, 5 mM glyoxylate, and 3 U of lactate dehydrogenase) and NADPH in various amounts. The reaction was started by the addition of NfnAB. After the reaction was started, the serum bottles were continuously shaken to secure H_2 transfer from the liquid phase into the gas phase. For H_2 quantification, 0.1-ml gas samples were withdrawn every 2 min and injected into a gas chromatography apparatus equipped with a Carlo Erba GC series 6000 thermal conductivity detector and a ShinCarbon ST micropacked column (Restek GmbH, Germany) (100/200 mesh; 1.0 mm by 2 m). N_2 was used as the carrier gas, and the flow rate was 60 ml per min. The temperatures of the detector and the oven were set at 143°C and 110°C, respectively. The amount of H_2 was calculated according to the standard curve correlated with peak areas.

RESULTS

The NAD$^+$-dependent formation of H_2 from NADPH and the NADH-dependent reduction of NADP$^+$ with H_2 catalyzed by cell extracts of *C. kluyveri* were proposed to involve a reduced ferredoxin:NADP$^+$ oxidoreductase, ferredoxin, and ferredoxin-dependent hydrogenase (21, 34). For the purification of the oxidoreductase, a photometric assay was looked for that would function in the presence of the hydrogenase but would not require the hydrogenase present in the cell extracts. The reduction of ferredoxin can be followed by photometrical observation at 430 nm ($\Delta\varepsilon_{ox\text{-}red} \approx$ 13.1 mM^{-1} cm^{-1}) without being interfered with by the absorbance changes below 400 nm that are associated with NAD(P)H oxidation and NAD(P)$^+$ reduction. However, in the presence of hydrogenase, reduced ferredoxin is rapidly oxidized, with concomitant formation of H_2. We therefore looked for an electron acceptor with a redox potential more positive than that of the hydrogen electrode at pH 7 ($E_o' = -414$ mV) that can substitute for ferredoxin ($E_o' = -420$ mV). We finally found that cell extracts of *C. kluyveri* catalyze an NAD$^+$-stimulated reduction with NADPH of triphenyltetrazolium chloride (TTC) ($E_o' = -80$ mV; $n = 2$) (10), which can be followed by photometrical observation at 546 nm. Stimulation of NADPH:TTC reductase activity by NAD$^+$ occurred at a 5-fold level. In the presence of NAD$^+$, the specific activity of TTC reduction using NADPH in cell extracts of *C. kluyveri* was approximately 0.8 U per mg.

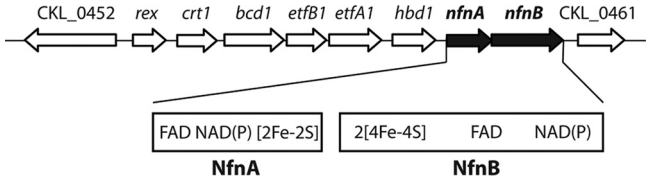

FIG. 1. The *Clostridium kluyveri* genomic region around the *nfnAB* genes and putative conserved domains of the two Nfn proteins. The third base in the stop codon (TAA) for *nfnA* overlaps with the first base of the start codon (ATG) for *nfnB*. The *nfnAB* gene is located downstream of *crt1-bcd1-etfAB1-hbd1* cluster, which is involved in butyryl-CoA formation from acetoacetyl-CoA and encodes 3-hydroxybutyryl-CoA dehydratase (*crt1*), the butyryl-CoA dehydrogenase-EtfAB complex (*bcd1-etfAB1*), and NADP$^+$-dependent β-hydroxybutyryl-CoA dehydrogenase (*hbd1*). *rex* is predicted to encode a redox-sensing transcriptional repressor that modulates transcription in response to the NADH/NAD$^+$ redox state.

Partial purification of the NfnAB from *C. kluyveri*. The NAD$^+$-dependent TTC reductase activity in the cell extracts was rapidly lost under oxic conditions. The activity was also rapidly lost upon dilution. This loss could be slowed down considerably by the addition of FAD at a 5 μM concentration. Flavin mononucleotide (FMN) could not substitute for FAD in this effect. But even under strictly anaerobic conditions and in the presence of FAD, purification was difficult. After chromatography, fractions had to be recombined for activity, indicating that the enzyme was composed of at least two different subunits that dissociated under the experimental conditions used.

For the fractions with activity, we used mass spectrometry to identify two polypeptides that are encoded by two open reading frames designated *nfnAB* (Fig. 1) and that form a transcription unit as determined by reverse transcription (RT)-PCR analysis (unpublished results). The upstream genes on the circular 3.96-Mbp chromosome (GenBank accession number CP000673) encode Rex (*rex* [CKL_0453]), crotonyl-CoA hydratase (*crt1*

[CKL_0454]), butyryl-CoA dehydrogenase (*bcd1* [CKL_0455]), EtfB (*etfB1* [CKL_0456]), EtfA (*etfA1* [CKL_0457]), and $NADP^+$-dependent β-hydroxybutyryl-CoA dehydrogenase (*hbd1* [CKL_0458]), all involved in the formation of butyryl-CoA from acetyl-CoA (Fig. 1). The open reading frame *nfnA* (CKL_0459) is predicted to encode a 32.6-kDa protein with binding sites for NAD(P), FAD, and a [2Fe2S] cluster with sequence similarity to ferredoxin:$NADP^+$ oxidoreductase from plants, and *nfnB* (CKL_0460) is predicted to encode a 49.8-kDa protein with binding sites for NAD(P), FAD, and two [4Fe4S] clusters with sequence similarity to the β subunit of $NADP^+$-dependent glutamate synthase (Fig. 1).

Heterologous expression of *nfnAB*, *nfnA*, and *nfnB*. To determine whether the *nfnA* and *nfnB* open reading frames encode the enzyme catalyzing the NAD^+-dependent reduction of TTC with NADPH in *C. kluyveri*, we cloned them alone and together into expression vectors for transformation of *E. coli*. After induction with IPTG, most of the recombinant protein was found in the inclusion body fraction but some could be recovered in the 40,000 × *g* supernatant, which catalyzed the (5-fold) NAD^+-stimulated reduction of TTC with NADPH at a specific activity of 0.4 to 0.5 U per mg of protein when the two open reading frames were expressed together. When *nfnA* and *nfnB* were individually expressed, most of the recombinant protein was also found in the inclusion body fraction. Only in the case of *nfnB* expression was there some NADPH:TTC oxidoreductase activity in the soluble fraction (0.06 U/mg), but this activity was not stimulated by NAD^+. However, when extracts of cells in which *nfnA* was expressed were mixed with extracts of cells in which *nfnB* was expressed, NAD^+-stimulated TTC reduction with NADPH was then observed, albeit only at a relatively low specific activity (~0.1 U/mg).

The extracts of *E. coli* cells in which both *nfnA* and *nfnB* were expressed catalyzed the NAD^+-dependent reduction of ferredoxin with NADPH at a specific activity of approximately 0.8 to 1 U per mg of protein. This activity was not observed in nonrecombinant *E. coli* cells or in cells in which only either *nfnA* or *nfnB* was expressed.

Purification of recombinant NfnAB, NfnA, and NfnB. For the purification of the recombinant enzyme on a nickel agarose column, only *nfnA* of the *nfnAB* transcription unit was first tagged with a 5′ His_6 cassette. N-terminal His tagging did not reduce inclusion body formation. Upon application of the cell extract to the nickel agarose column, NfnB was recovered in the flow-through fractions and only NfnA protein was retained. The NfnA protein was subsequently eluted with imidazole. Almost the same results were obtained when only *nfnB* of the *nfnAB* transcription unit was provided with a 3′-terminal His_6 cassette.

We therefore constructed a transcription vector in which *nfnA* carried a 5′ His_6 cassette and *nfnB* a 3′ His_6 cassette. Both subunits of the recombinant enzyme were now retained on nickel agarose and eluted with imidazole as represented by one broad activity peak containing NfnA and NfnB in an almost 1-to-1 ratio, as judged from a scan of the Coomassie brilliant blue-stained SDS-PAGE gels.

The purified NfnAB complex had a specific activity at 37°C of between 3 and 6 U per mg of protein in the presence of NAD^+ in the TTC reduction assay and contained between 3 and 5 mol of iron per assumed heterodimer. The values differed from preparation to preparation. In the absence of NAD^+, only 25% of the specific activity was found.

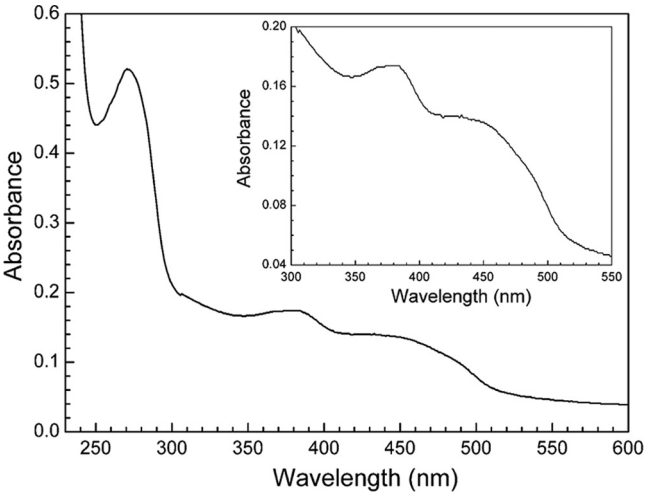

FIG. 2. The UV-visible absorption spectrum of purified recombinant NfnAB after *in vitro* FeS cluster reconstitution. The sample contained 1.2 mg of protein/ml in 50 mM Tris-HCl (pH 7.4). An enlargement of the spectrum from 300 nm to 550 nm is shown in the inset.

FeS cluster reconstitution. The specific activity of purified NfnAB in the presence of NAD^+ (TTC assay) increased up to 10 U per mg when the purified enzyme complex was incubated in the presence of FAD (10 μM), Fe^{2+} (1.5 mM), cysteine (2 mM), and 8 mM DTT at pH 7.4 for 1 h at room temperature before being measured. Inclusion of Na_2S in the FeS cluster reconstitution assay was not necessary, probably because of the presence of HS^- formed from cysteine and DTT under the assay conditions. After removal of nonbound Fe^{2+} by ultrafiltration, the preparations with the UV-visible spectrum shown in Fig. 2 contained up to 10 Fe molecules per heterodimer, which is consistent with the presence of two [4Fe4S] and one [2Fe2S] clusters (Fig. 1). An analysis of the exact FAD content was not possible, because FAD had to be added to all the solutions for the enzyme to retain activity.

We also reconstituted the FeS clusters in purified NfnA and NfnB. After the free iron and sulfur sources were removed by ultrafiltration, NfnA was found to contain about 1.7 mol of Fe per mol of protein and NfnB about 6 mol of Fe per mol of protein, which was less than was predicted based on the sequence (Fig. 1). Only NfnB contained bound FAD in detectable amounts.

Activities exhibited by NfnAB. Besides the observed NAD^+-stimulated reduction of TTC with NADPH, the purified enzyme complex catalyzed the NAD^+-dependent reduction of ferredoxin with NADPH, the ferredoxin-dependent reduction of NAD^+ with NADPH, the NADH-dependent reduction of $NADP^+$ with reduced ferredoxin, the reduction of benzyl viologen with NADPH and NADH, and the oxidation of NADPH and NADH with O_2. The results reported below and in Table 1 are those for the FeS cluster reconstituted enzyme complex with a specific activity in the NADPH:TTC oxidoreductase assay of 8 U/mg in the presence of NAD^+.

In the assays, ferredoxin from *C. pasteurianum* rather than from *C. kluyveri* was employed because ferredoxin from *C.*

TABLE 1. Reactions catalyzed by NfnAB from *Clostridium kluyveri* after FeS cluster reconstitution[a]

Reaction	Apparent K_m[h] (mM)	Apparent V_{max} (U/mg)
NADPH[b]→TTC (NAD$^+$ stimulated)	0.001 (NADPH) 0.01 (NAD$^+$)	2 (− NAD$^+$) 8 (+ NAD$^+$)
NADPH[b]→Fd_{ox} (NAD$^+$ dependent)	0.025 (NADPH) 1[e] (NAD$^+$)	0.1 (− NAD$^+$) 23 (+ NAD$^+$)
NADPH[b]→NAD$^+$ (Fd_{ox}[c] dependent)	0.001 (NADPH) 2 (NAD$^+$)	<0.1 (− Fd) 8 (+ Fd_{ox}[c]) 4.4 (+ Fd_{red}[d])
Fd_{red}[d]→NADP$^+$ (NADH dependent)	0.1 (NADP$^+$) 0.01 (NADH)	0.2 (− NADH) 28 (+ NADH) <0.01 (− Fd)
NADH→NADP$^+$ (Fd_{red}[d] dependent)	0.01 (NADH) 0.1 (NADP$^+$)	<0.01 (− Fd) 28 (+ Fd_{red}[d]) <0.01 (+ Fd_{ox}[c])
NADPH[b]→benzyl viologen	0.001 (NADPH) 0.015 (benzyl viologen)	15 (− NAD$^+$) 24 (+ NAD$^+$)[f]
NADH→benzyl viologen		0.6 (− NADP$^+$) 0.1 (+ NADP$^+$)[g]
NADPH→O_2		5.6 (− NAD$^+$) 20 (+ NAD$^+$)[i]
NADH→O_2		1 (− NADP$^+$) 0.4 (+ NADP$^+$)

[a] Ferredoxin was present only where indicated.
[b] NADPH regeneration system (glucose-6-phosphate dehydrogenase and glucose-6-phosphate).
[c] Fd_{ox} regeneration system (hydrogenase and 100% N_2).
[d] Fd_{red} regeneration system (hydrogenase and 100% H_2), keeping the ferredoxin about 50% reduced.
[e] An apparent K_m for NAD$^+$ of 0.1 mM was determined for cell extracts of *C. kluyveri* (34).
[f] 2 mM NAD$^+$.
[g] 2 mM NADP$^+$.
[h] Extrapolated from Lineweaver-Burk plots and rounded.
[i] NAD$^+$ regeneration system (lactate dehydrogenase and pyruvate).

pasteurianum is easier to purify in the amounts required. The two ferredoxins are very similar, as indicated by sequence identity of >60%, and it is know that ferredoxins from different organisms can substitute for one another (29).

The NAD$^+$-dependent reduction of ferredoxin with NADPH (continuously regenerated) was measured by following the decrease in ferredoxin absorbance at 430 nm. In the absence of NAD$^+$, ferredoxin was only very slowly reduced (0.5% of the rate seen in the presence of NAD$^+$). The apparent K_m for NAD$^+$ was found to be approximately 1 mM and for NADPH to be 25 μM, and the apparent V_{max} was found to be 23 U per mg of protein at pH 7 and 37°C. The pH optimum was near 7 (Table 1).

The ferredoxin-dependent reduction of NAD$^+$ with NADPH (continuously regenerated) could be followed by photometrical observations at 380 nm ($\varepsilon = 1.2$ mM^{-1} cm^{-1}) only when the assays were supplemented with hydrogenase from *C. pasteurianum* (1 U) to keep the ferredoxin mainly in its oxidized state. Otherwise, the increase in absorbance accompanying NADH formation was not seen due to the decrease in absorbance at 380 nm accompanying ferredoxin reduction ($\Delta\varepsilon_{ox\text{-}red} \approx 8.6$ mM^{-1} cm^{-1}). But even in the presence of hydrogenase, some ferredoxin was always reduced. Therefore, the specific activity of ferredoxin-dependent NAD$^+$ reduction with NADPH could not be accurately determined. The specific activity obtained was 8 U per mg of protein, which is one-third the amount expected on the basis of the stoichiometry analysis of reaction 5. With the assay, however, it could be unambiguously shown that, in the absence of ferredoxin, NAD$^+$ was only very slowly reduced (<1% of the rate observed in the presence of ferredoxin) (Table 1).

The NADH-dependent reduction of NADP$^+$ with reduced ferredoxin was followed by photometrical observations at 380 nm. Reduced ferredoxin was continuously regenerated via the presence of H_2 (at 10^5 Pa) and hydrogenase. In the absence of ferredoxin, no NADP$^+$ was reduced with NADH. The apparent K_m for NADH was found to be approximately 10 μM and for NADP$^+$ to be approximately 0.1 mM, and the apparent V_{max} was found to be 28 U per mg of protein at 37°C and pH 7. In the absence of NADH, the apparent V_{max} for NADP$^+$ reduction with reduced ferredoxin was 0.2 U/mg (Table 1).

The purified enzyme complex catalyzed the reduction of benzyl viologen with NADPH in the absence (15 U/mg) and presence (24 U/mg) of NAD$^+$ and the reduction of benzyl viologen with NADH in the absence (0.6 U/mg) and presence (0.1 U/mg) of NADP$^+$ (Table 1).

NfnAB catalyzed the NAD$^+$-stimulated oxidation of NADPH with O_2 (20 U/mg) and the oxidation of NADH (1 U/mg) (Table 1). During catalysis, the enzyme was inactivated.

Activities exhibited by NfnA and NfnB. Whereas purified NfnA did not catalyze the reduction of TTC with NADPH in the absence or presence of NAD$^+$, purified NfnB did (0.4 U/mg). TTC reduction catalyzed by NfnB was not stimulated by NAD$^+$. When purified NfnA and NfnB were mixed in an optimal ratio of 1 to 1, however, the resulting complex then showed NAD$^+$-stimulated NADPH:TTC oxidoreductase activity (0.9 U/mg).

With both NADPH and NADH, purified NfnA showed very little benzyl viologen-reducing activity (0.05 U/mg with NADPH with or without NAD$^+$ and 0.01 U/mg with NADH with or without NADP$^+$). Purified NfnB catalyzed the reduction of benzyl viologen with NADPH with or without NAD$^+$ at a specific activity of approximate 2 U/mg and with NADH at a specific activity of 0.01 U/mg (with NADP$^+$) or 0.07 U/mg (without NADP$^+$).

Stoichiometry of NfnAB-catalyzed reactions. The following stoichiometry results were determined: (i) moles of ferredoxin reduced by NADPH per mole of NAD$^+$ reduced (backward reaction 5); (ii) moles of ferredoxin reduced by NADPH per mole of NADPH oxidized (backward reaction 5); and (iii) moles of NADP$^+$ reduced by reduced ferredoxin and NADH per mole of NADH oxidized (forward reaction 5).

In order to determine the moles of ferredoxin reduced per mole of NAD$^+$ reduced, the NADPH/NADP$^+$ ratio in the assay was kept high (above 100 to 1) via an NADPH regeneration system and the moles of ferredoxin reduced per mole of NAD$^+$ added were measured. Ferredoxin reduction was followed by measurement of the formation of H_2 in the presence of hydrogenase from *C. pasteurianum*. Approximately 1 mol of H_2 was formed per mol of NAD$^+$ added (Fig. 3A).

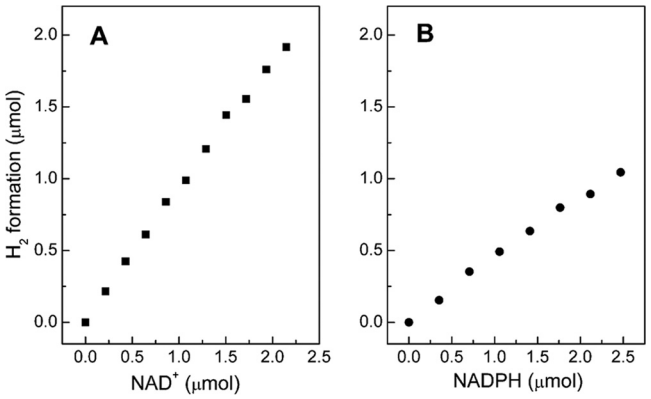

FIG. 3. NAD^+-dependent H_2 formation from NADPH catalyzed by purified recombinant NfnAB in the presence of ferredoxin and hydrogenase. (A) Amount of H_2 formed as a function of the amount of NAD^+ added in the presence of an NADPH regeneration system. (B) Amount of H_2 formed as a function of the amount of NADPH added in the presence of an NAD^+ regeneration system. The reactions were started with NfnAB (270 μg); then, 0.1-ml gas samples were withdrawn at 2-min intervals for the determination of the amount of H_2 formed via gas chromatography analysis. The values for H_2 plotted on the ordinate represent the amounts obtained after the reaction had completely finished. The slopes depicted in panels A and B indicate that approximately 1.1 μmol of NAD^+ (A) and 2.2 μmol of NADPH (B) were required for the formation of 1 μmol of H_2 in the presence of excess NADPH (A) and NAD^+ (B), respectively.

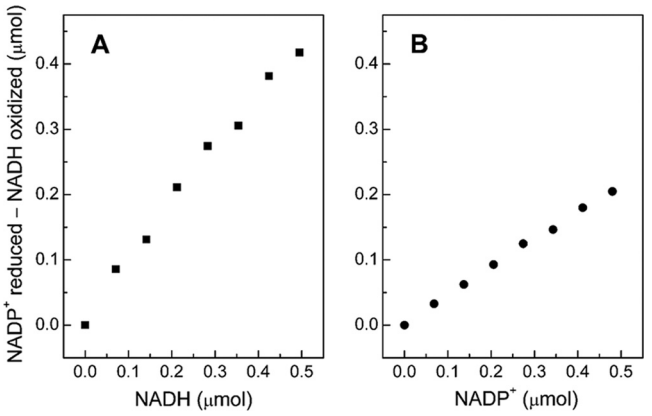

FIG. 4. NADH-dependent $NADP^+$ reduction with reduced ferredoxin catalyzed by purified recombinant NfnAB (40 μg) in the presence of hydrogenase and H_2. (A) Amount of $NADP^+$ reduced minus the amount of NADH oxidized as a function of the amount of NADH added in the presence of excess amounts of $NADP^+$ (2 mM). (B) Amount of $NADP^+$ reduced minus the amount of NADH oxidized as a function of the amount of $NADP^+$ added in the presence of excess amounts of NADH (0.5 mM). The reaction was started with $NADP^+$ and was followed by photometrical observations at 380 nm (for both NADPH and NADH, $\varepsilon_{380} = 1.2\ mM^{-1}\ cm^{-1}$). The difference between the amount of $NADP^+$ reduced and the amount of NADH oxidized was calculated based on the absorbance change after the reaction had completely finished. The slopes in panels A and B indicate that approximately 0.11 μmol of NADH (A) and 0.22 μmol of $NADP^+$ (B) were required for the formation of 0.10 μmol of NAD(P)H in the presence of excess $NADP^+$ (A) and NADH (B), respectively.

In order to determine the moles of ferredoxin reduced per mole of NADPH oxidized (backward reaction 5), the moles of ferredoxin reduced per mole of NADPH added in the presence of excess NAD^+ were determined. Ferredoxin reduction was followed via measurement of the formation of H_2 in the presence of hydrogenase. Approximately 0.5 mol of H_2 was formed per mol of NADPH added (Fig. 3B).

For the determination of the moles of $NADP^+$ reduced per mole of NADH oxidized in the forward reaction, the concentration of reduced ferredoxin in the assay was kept constant (50% reduced) via a reduced ferredoxin regeneration system (hydrogenase and H_2 at 10^5 Pa). Approximately 2 mol of $NADP^+$ per mol of NADH added was found to be reduced as deduced from the increase in absorbance at 380 nm, exploiting the fact that NADH and NADP have identical extinction coefficients at 380 nm (Fig. 4A). As a control, using the same method, it was shown that 1 mol of $NADP^+$ was reduced by reduced ferredoxin and NADH per mol of $NADP^+$ added to the assay (Fig. 4B).

The observed stoichiometry results were reproducible with different batches of purified NfnAB and were independent of the specific activity seen after reconstitution of the FeS clusters.

DISCUSSION

The results clearly indicate that the cytoplasmic NfnAB complex from *C. kluyveri* catalyzes reaction 5. The UV-visible spectrum of the complex (Fig. 2) is indicative of the presence of an iron-sulfur flavoprotein that most probably harbors two [4Fe4S] clusters, one [2Fe2S] cluster, and two FADs per heterodimer (Fig. 1), although the exact stoichiometry data remain to be determined. Coupling of the endergonic reduction of $NADP^+$ with NADH to the exergonic reduction of $NADP^+$ with reduced ferredoxin thus most likely proceeds via flavin-based electron bifurcations, as proposed in Fig. 5. This is probably the only way for *C. kluyveri* to regenerate NADPH from NADH and $NADP^+$, since an open reading frame for a proton-translocating transhydrogenase is not found in its genome (27); in other bacteria, e.g., *E. coli*, the proton-translocating transhydrogenase catalyzes the energy-dependent $NADP^+$ reduction with NADH (18).

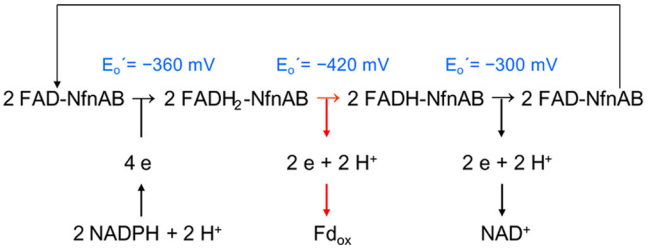

FIG. 5. Proposed flavin-based electron bifurcation (in red) involved in the reversible reduction of ferredoxin (Fd) and NAD^+ with two NADPHs as catalyzed by the NfnAB complex from *Clostridium kluyveri.* Only the direction of ferredoxin and NAD^+ reduction with NADPH is shown. The standard E_o' redox potentials of the three FAD_{ox}/FAD_{red} couples were arbitrarily chosen so as to conform to the first law of thermodynamics. The E_o' of the FAD/FADH couple, when free in solution, is −205 mV (4). The 155-mV (more negative) E_o' of the FAD/$FADH_2$ couple shown when it is bound to the protein can be explained by assuming that FAD binds approximately 10^5 times more tightly to the protein than $FADH_2$.

Unfortunately, until now, the NfnAB complex could be reconstituted from separately produced NfnA and NfnB with very low specific activity. Whereas heterologously produced NfnB contained bound FAD after dialysis and showed some diaphorase activity with NADPH, NfnA did not contain bound FAD and was essentially inactive. The diaphorase activity of NfnB was much higher with NADPH than with NADH, indicating that NfnB harbors an NADP binding site.

Flavin-based electron bifurcation was first proposed for the coupling of the endergonic reduction of ferredoxin with NADH to the exergonic reduction of crotonyl-CoA with NADH as catalyzed by the butyryl-CoA dehydrogenase-EtfAB complex (reaction 2) (7, 12). Two other recent examples of putative flavin-based electron bifurcations are the coupling of the exergonic reduction of the heterodisufide CoM-S-S-CoB with H_2 with the endergonic reduction of ferredoxin with H_2 as catalyzed by the MvhADG/HdrABC complex from methanogenic archaea (32, 33) and the coupling of the exergonic formation of H_2 from reduced ferredoxin with the endergonic formation of H_2 from NADH as catalyzed by the heterotrimeric [FeFe] hydrogenases from *Thermotoga maritima* (25). The NfnAB complex has in common with these other complexes the fact that it contains FAD (in the case of the [FeFe] hydrogenase from *T. maritima* FMN) that is loosely bound only when in the reduced form, resulting in a gradual loss of activity in the absence of added FAD (FMN).

The protein-encoding sequences for NfnAB are found in the genomes of many other *Clostridium spp.*, one exception being *C. acetobutylicum.* They are also present in many other Gram-positive genera, namely, *Eubacterium*, *Thermoanaerobacter*, *Anaerococcus*, *Anaerocellum*, *Carboxydothermus*, and *Desulfotomaculum*. But the *nfnAB* genes are also found outside this group, e.g., in some *Dictyoglomus*, *Bacteroides*, *Thermotoga*, *Pyrococcus*, *Thermococcus*, and *Methanosarcina* species. NfnAB has been purified from *P. furiosus*. The enzyme was first considered to be a sulfide dehydrogenase (15) but was later thought to function *in vivo* as reduced ferredoxin:NADP oxidoreductase (14, 26). Whether the enzyme catalyzes reaction 5 was not determined.

C. kluyveri has been shown to contain an NADP$^+$- and NAD$^+$-dependent β-hydroxybutyryl-CoA dehydrogenase (Hbd1 and Hbd2), indicating an involvement of NADPH and thus of NfnAB in acetyl-CoA reduction to butyryl-CoA (27). The specific activity of purified NfnAB was 28 U of NADP$^+$ reduced per mg of protein (Table 1). The specific activity of NADH-dependent NADP$^+$ reduction with H_2 in cell extracts of *C. kluyveri* is approximately 10-fold lower (2 U per mg of protein) but is high enough for the enzyme to have a catabolic function. The specific rate of butyrate formation from ethanol and acetate in cell suspensions of *C. kluyveri* has been determined to be approximately 0.3 U per mg of protein (19), which is roughly 1% of the specific activity of the NfnAB complex.

The fermentation of 6 ethanol and 3 acetate molecules to 3 butyrate, 1 caproate, 1 H^+, and 2 H_2 molecules (reaction 1) is exergonic (−183.5 kJ/mol H^+) ($\Delta G^{o\prime}$) when all substrates and products are at 1 M concentrations and protons are at pH 7. The free-energy change ($\Delta G'$) is considerably lower when the substrate and product concentrations are lower than 1 M due to the fact that 9 substrates are converted to only 4 products (reaction 1); e.g., at 100 mM concentrations of substrates and products, the free-energy change is −155 kJ/mol H^+ and at 1 mM only −100 kJ/mol H^+, levels sufficient to drive the synthesis of approximately 2.5 and 1.5 mol of ATP, respectively, considering that 60 to 80 kJ per mol is required *in vivo* for the phosphorylation of one ADP molecule (30).

We show in Fig. 6 how the fermentation could be coupled with the formation of 1.25 ATP at 1 mM concentrations of ethanol, acetate, and butyrate ($\Delta G' = -100$ kJ/mol H^+) involving NfnAB. For simplification purposes, it was assumed that only butyrate rather than caproate is formed, which is indeed the case when the butyrate concentration is low at the beginning of the fermentation. Coupling involves both substrate-level phosphorylation (1 ATP) and electron transport phosphorylation (0.25 ATP) via RnfABCDEG and F_1F_0-ATP synthetase. The reduced ferredoxin required for electrogenic proton translocation via RnfABCDEG is provided in the butyryl-CoA dehydrogenase-EtfAB reaction via flavin-based electron bifurcation. Of the 5 reduced ferredoxins, 2 are reoxidized in the HydA-catalyzed reaction, 2.5 in the NfnAB-catalyzed reaction, and 0.5 in the RnfABCDEG-catalyzed reaction. Under these conditions, only the NADP$^+$-dependent β-hydroxybutyryl-CoA dehydrogenase (Hbd1) is functional (Fig. 6).

When the concentrations of ethanol, acetate, and butyrate are higher than 1 mM and the free-energy change thus permits the synthesis of more than 1.25 mol of ATP, all that has to happen is that the percentage of reduced ferredoxin reoxidized in the RnfABCDEG-catalyzed reaction is increased and the percentage in the NfnAB-catalyzed reaction is decreased (Fig. 6). As a consequence, more NADH is generated than is oxidized during butyryl-CoA formation from acetyl-CoA that involves only NADP$^+$-dependent β-hydroxybutyryl-CoA dehydrogenase (Hbd1), as shown in Fig. 6. Therefore, to balance the NADH budget, the NAD$^+$-dependent β-hydroxybutyryl-CoA dehydrogenase (Hbd2) then has to become functional (not shown).

How the energy and redox status in *C. kluyveri* is sensed and adjusted is not yet known. Interestingly, the *nfnAB* transcription unit lies downstream of five protein coding sequences (CDS) for enzymes involved in butyric acid formation (Fig. 1). These five CDS are preceded by an open reading frame for a Rex redox-sensing transcriptional repressor. The Rex protein has been implicated in the regulation of the expression of genes important for fermentative growth and for growth under conditions of low oxygen tension in many Gram-positive bacteria but is also found in some bacteria outside this group, e.g., in *Thermus* species (1, 5, 6, 28). Rex senses the redox poise of the cell through changes in the NADH/NAD$^+$ ratio, with an increase in the ratio leading to a derepression and a decrease to a repression of gene expression. Repression is mediated by binding of Rex to the promoter region, with binding becoming tighter at low NADH/NAD$^+$ ratios and less tight at high NADH/NAD ratios. The operator sequence to which Rex binds has been mapped and has been shown in the case of *Bacillus subtilis* to be an AT-rich 20-bp palindromic sequence. This sequence can significantly differ between different organisms both in length and in the completeness of the palindrome. This is reflected in significantly different primary structures of the Rex proteins from different organisms (1, 6, 17, 22, 28, 35). Thus, it is difficult to determine to which promoter the Rex

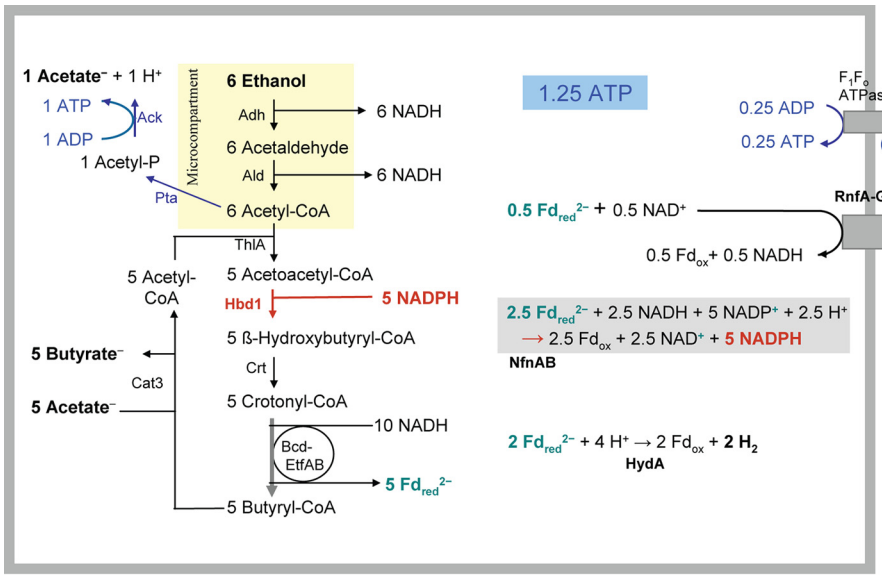

6 Ethanol + 4 Acetate⁻ → 5 Butyrate⁻ + 1 H⁺ + 4 H_2O + 2 H_2 ΔG´= −100 kJ/mol (1 mM)

FIG. 6. Scheme of the ethanol-acetate fermentation of *Clostridium kluyveri* at 1 mM concentrations of ethanol, acetate, and butyrate, highlighting the role of NfnAB (the reaction is indicated with a gray-shaded box). The free-energy change of −100 kJ/mol permits the synthesis of 1 to 1.5 mol of ATP (see text). To obtain this ATP gain, for the 5 mol of ferredoxin (Fd) reduced in the butyryl-CoA dehydrogenase reaction (catalyzed by the Bcd-EtfAB complex), 2 mol of Fd_{red}^{2-} must be reoxidized by protons in the HydA-catalyzed hydrogenase reaction, 2.5 mol of Fd_{red}^{2-} by $NADP^+$ in the NfnAB-catalyzed reaction, and 0.5 mol of Fd_{red}^{2-} by NAD^+ in the RnfABCDEG-catalyzed reaction. The nature of the involvement of the RnfA-G complex and the coupling cation is still speculative.

protein from *C. kluyveri* actually binds; this would therefore have to be experimentally determined.

The new electron-bifurcating enzyme described in this report thus gives a new perspective for our understanding of the bioenergetics and mechanism of ferredoxin-dependent reactions in *C. kluyveri* and of anaerobic metabolism in general (25).

ACKNOWLEDGMENTS

This work was supported by the Max Planck Society and by the Fonds der Chemischen Industrie.

We thank Jörg Kahnt for MALDI-TOF MS analyses.

REFERENCES

1. **Brekasis, D., and M. S. B. Paget.** 2003. A novel sensor of NADH/NAD^+ redox poise in *Streptomyces coelicolor* A3(2). EMBO J. **22:**4856–4865.
2. **Decker, K., and S. Pfitzer.** 1972. Determination of steady-state concentrations of adenine nucleotides in growing *C. kluyveri* cells by biosynthetic labeling. Anal. Biochem. **50:**529–539.
3. **Dickert, S., A. J. Pierik, D. Linder, and W. Buckel.** 2000. The involvement of coenzyme A esters in the dehydration of (*R*)-phenyllactate to (*E*)-cinnamate by *Clostridium sporogenes*. Eur. J. Biochem. **267:**3874–3884.
4. **Draper, R. D., and L. L. Ingraham.** 1968. A potentiometric study of the flavin semiquinone equilibrium. Arch. Biochem. Biophys. **125:**802–808.
5. **Du, X., and J. J. Pène.** 1999. Identification, cloning and expression of p25, an AT-rich DNA-binding protein from the extreme thermophile, Thermus aquaticus YT-1. Nucleic Acids Res. **27:**1690–1697.
6. **Gyan, S., Y. Shiohira, I. Sato, M. Takeuchi, and T. Sato.** 2006. Regulatory loop between redox sensing of the NADH/NAD^+ ratio by Rex (YdiH) and oxidation of NADH by NADH dehydrogenase Ndh in *Bacillus subtilis*. J. Bacteriol. **188:**7062–7071.
7. **Herrmann, G., E. Jayamani, G. Mai, and W. Buckel.** 2008. Energy conservation via electron-transferring flavoprotein in anaerobic bacteria. J. Bacteriol. **190:**784–791.
8. **Hillmer, P., and G. Gottschalk.** 1972. Particulate nature of enzymes involved in fermentation of ethanol and acetate by *Clostridium kluyveri*. FEBS Lett. **21:**351–354.
9. **Hillmer, P., and G. Gottschalk.** 1974. Solubilization and partial characterization of particulate dehydrogenases from *Clostridium kluyveri*. Biochim. Biophys. Acta **334:**12–23.
10. **Jerchel, D., and W. Mohle.** 1944. The determination of reduction potential of tetrazolium compounds. Ber. Deutsch. Chem. Ges. B **77:**591–601. (In German.)
11. **Jungermann, K., R. K. Thauer, G. Leimenstoll, and K. Decker.** 1973. Function of reduced pyridine nucleotide-ferredoxin oxidoreductases in saccharolytic clostridia. Biochim. Biophys. Acta **305:**268–280.
12. **Li, F., J. Hinderberger, H. Seedorf, J. Zhang, W. Buckel, and R. K. Thauer.** 2008. Coupled ferredoxin and crotonyl coenzyme A (CoA) reduction with NADH catalyzed by the butyryl-CoA dehydrogenase/Etf complex from *Clostridium kluyveri*. J. Bacteriol. **190:**843–850.
13. **Lurz, R., F. Mayer, and G. Gottschalk.** 1979. Electron microscopic study on the quaternary structure of the isolated particulate alcohol-acetaldehyde dehydrogenase complex and on its identity with the polygonal bodies of *Clostridium kluyveri*. Arch. Microbiol. **120:**255–262.
14. **Ma, K., and M. W. W. Adams.** 2001. Ferredoxin:NADP oxidoreductase from *Pyrococcus furiosus*. Methods Enzymol. **334:**40–45.
15. **Ma, K., and M. W. W. Adams.** 1994. Sulfide dehydrogenase from the hyperthermophilic archaeon *Pyrococcus furiosus*: a new multifunctional enzyme involved in the reduction of elemental sulfur. J. Bacteriol. **176:**6509–6517.
16. **Madan, V. K., P. Hillmer, and G. Gottschalk.** 1973. Purification and properties of NADP-dependent L(+)-3-hydroxybutyryl-CoA dehydrogenase from *Clostridium kluyveri*. Eur. J. Biochem. **32:**51–56.
17. **Nakamura, A., A. Sosa, H. Komori, A. Kita, and K. Miki.** 2007. Crystal structure of TTHA1657 (AT-rich DNA-binding protein; p25) from *Thermus thermophilus* HB8 at 2.16 Å resolution. Proteins **66:**755–759.
18. **Pedersen, A., G. B. Karlsson, and J. Rydström.** 2008. Proton-translocating transhydrogenase: an update of unsolved and controversial issues. J. Bioenerg. Biomembr. **40:**463–473.
19. **Pfeiff, B.** 1991. Untersuchungen zur Kopplung von H_2-Bildung und Fettsäuresynthese in *Clostridium kluyveri.* (Investigations of the coupling of H_2 formation and butyric acid/caproic acid synthesis in *Clostridium kluyveri.*) Diplom thesis. Philipps University, Marburg, Germany.
20. **Pierik, A. J., R. B. G. Wolbert, P. H. A. Mutsaers, W. R. Hagen, and C. Veeger.** 1992. Purification and biochemical characterization of a putative [6Fe-6S] prismane-cluster-containing protein from *Desulfovibrio vulgaris* (Hildenborough). Eur. J. Biochem. **206:**697–704.
21. **Rupprecht, E., and R. K. Thauer.** 1972. Mechanism and regulation of NADPH ferredoxin reductase from *Clostridium kluyveri*. Zentralbl. Bakteriol. Orig. A **220:**416–419. (In German.)
22. **Schau, M., Y. Chen, and F. M. Hulett.** 2004. *Bacillus subtilis* YdiH is a direct negative regulator of the *cydABCD* operon. J. Bacteriol. **186:**4585–4595.
23. **Schoberth, S., and G. Gottschalk.** 1969. Considerations on energy metabolism of *Clostridium kluyveri*. Arch. Mikrobiol. **65:**318–328. (In German.)

24. **Schönheit, P., C. Wäscher, and R. K. Thauer.** 1978. Rapid procedure for purification of ferredoxin from clostridia using polyethyleneimine. FEBS Lett. **89:**219–222.
25. **Schut, G. J., and M. W. W. Adams.** 2009. The iron-hydrogenase of *Thermotoga maritima* utilizes ferredoxin and NADH synergistically: a new perspective on anaerobic hydrogen production. J. Bacteriol. **191:**4451–4457.
26. **Schut, G. J., S. L. Bridger, and M. W. W. Adams.** 2007. Insights into the metabolism of elemental sulfur by the hyperthermophilic archaeon *Pyrococcus furiosus*: characterization of a coenzyme A-dependent NAD(P)H sulfur oxidoreductase. J. Bacteriol. **189:**4431–4441.
27. **Seedorf, H., W. F. Fricke, B. Veith, H. Brüggemann, H. Liesegang, A. Strittimatter, M. Miethke, W. Buckel, J. Hinderberger, F. Li, C. Hagemeier, R. K. Thauer, and G. Gottschalk.** 2008. The genome of *Clostridium kluyveri*, a strict anaerobe with unique metabolic features. Proc. Natl. Acad. Sci. U. S. A. **105:**2128–2133.
28. **Sickmier, E. A., D. Brekasis, S. Paranawithana, J. B. Bonanno, M. S. B. Paget, S. K. Burley, and C. L. Kielkopf.** 2005. X-ray structure of a Rex-family repressor/NADH complex insights into the mechanism of redox sensing. Structure **13:**43–54.
29. **Tagawa, K., and D. I. Arnon.** 1962. Ferredoxins as electron carriers in photosynthesis and in the biological production and consumption of hydrogen gas. Nature **195:**537–543.
30. **Thauer, R. K., K. Jungermann, and K. Decker.** 1977. Energy conservation in chemotropic anaerobic bacteria. Bacteriol. Rev. **41:**100–180.
31. **Thauer, R. K., K. Jungermann, H. Henninger, J. Wenning, and K. Decker.** 1968. Energy metabolism of *Clostridium kluyveri*. Eur. J. Biochem. **4:**173–180.
32. **Thauer, R. K., A. Kaster, M. Goenrich, M. Schick, T. Hiromoto, and S. Shima.** 2010. Hydrogenases from methanogenic archaea: structure and function, nickel regulation, and H_2-storage. Annu. Rev. Biochem. **2010:**507–536.
33. **Thauer, R. K., A. K. Kaster, H. Seedorf, W. Buckel, and R. Hedderich.** 2008. Methanogenic archaea: ecologically relevant differences in energy conservation. Nat. Rev. Microbiol. **6:**579–591.
34. **Thauer, R. K., E. Rupprecht, C. Ohrloff, K. Jungermann, and K. Decker.** 1971. Regulation of reduced nicotinamide adenine dinucleotide phosphate-ferredoxin reductase system in *Clostridium kluyveri*. J. Biol. Chem. **246:**954–959.
35. **Wang, E., M. C. Bauer, A. Rogstam, S. Linse, D. T. Logan, and C. von Wachenfeldt.** 2008. Structure and functional properties of the *Bacillus subtilis* transcriptional repressor Rex. Mol. Microbiol. **69:**466–478.